Investigating candidate genes for an association with skin color pattern in the mimic poison frog, *Ranitomeya imitator*

By

Emily D. White

July, 2020

Director of Thesis: Kyle Summers, PhD

Major Department: Biology

Understanding the genetic basis of adaptive traits can help us better understand their evolution. The mimic poison frog, *Ranitomeya imitator,* is native to Peru. Like many other species of poison frogs, it has aposematic coloration to warn predators of its toxicity, so that its dorsal color pattern is directly linked to its survival. Recently, *R. imitator* has undergone a mimetic radiation, in which it has evolved to mimic three species of congeneric poison frogs. This mimicry has caused a divergence of color pattern within *R. imitator*, giving rise to four different color pattern morphs (striped, spotted, banded, and varadero). In this thesis, the main objective is to investigate the genetic basis of this phenotypic divergence. Here, we focus specifically on investigating candidate color pattern genes in the striped and banded morphs, which differ mainly in their dorsal color (yellow to orange), hindlimb color (green to orange), and their dorsal pattern (striped to banded). To do this, we formed a lab-reared pedigree by crossing two morphs of *R. imitator* (striped and banded) for two generations. For each individual in the pedigree, we amplified each candidate gene (*asip, mc1r, bsn,* and *retsat*) and sequenced them via Sanger sequencing. To determine phenotypes, we took spectral reflectance measurements and photos of each frog. We analyzed and summarized spectral reflectance data using the PAVO package in R. The photos were analyzed using a program written by Tyler Linderoth, which quantifies the orientation of the dorsal stripes/bands. We used the program Merlin to test for a genotype-phenotype association. Our tests indicated associations between genotype and color pattern phenotypes for all four candidate genes tested. Our results show that these genes are promising

candidates for controlling aspects of skin color pattern in *R. imitator*. Further study of these genes will help elucidate the proximate mechanisms of phenotypic divergence in *R. imitator,* giving us a better understanding of the evolution of aposematism in this species and potential insights into the molecular basis of skin color pattern more generally.

Investigating candidate genes for an association with skin color pattern in the mimic poison frog *Ranitomeya imitator*

A Thesis

Presented to the Faculty of the Department of Biology

At East Carolina University

In Partial Fulfillment of the Requirements for the Degree

Master of Science in Biology

By

Emily D. White

July, 2020

Investigating candidate genes for an association with skin color pattern in the mimic poison frog *Ranitomeya imitator*

By

Emily White

APPROVED BY:

DIRECTOR
OF THESIS: _____
Kyle Summers, PhD

COMMITTEE
MEMBER: _____
Trip Lamb, PhD

COMMITTEE
MEMBER: _____
Michael S. Brewer II, PhD

CHAIR OF THE
DEPARTMENT
OF BIOLOGY: _____
David Chalcraft, PhD

DEAN OF THE
GRADUATE SCHOOL: _____
Paul J. Gemperline, PhD

ACKNOWLEDGEMENTS

First and foremost, I extend my sincere thanks to my advisor, Dr. Kyle Summers, for his guidance and support throughout this work. I would also like to thank my committee members, Dr. Trip Lamb and Dr. Michael Brewer for their helpful feedback and advice along the way. Additionally, I would like to thank Tyler Linderoth and Adam Stuckert for their help with various aspects of this project. Finally, I am grateful for the consistent encouragement and companionship that my lab mates, friends, and family have given me throughout this process.

TABLE OF CONTENTS

LIST OF TABLES

LIST OF FIGURES

INTRODUCTION

Identifying the molecular basis of ecologically important traits is key to understanding how they evolve. Color pattern is one such trait that is ecologically important and of significant interest to evolutionary biologists, especially because of the many roles it plays in animal signaling, camouflage, mimicry, and thermoregulation. It is intimately linked with survival and reproduction and directly affects fitness in many species. One prime example of this is aposematism, where toxic prey evolve bright coloration as a warning signal to deter predation.

In some cases, aposematic color pattern may diverge within a species, as is the case with the mimic poison frog *Ranitomeya imitator*. Four different color pattern morphs (striped, spotted, banded, and varadero) have diverged within this species. This divergence is due to Mullerian mimicry, which has caused *R. imitator* to share color patterns with three other species of poison frogs, one of which has two morphs itself (Symula, Schulte, and Summers 2001). Mullerian mimicry can be caused by the concurrent phenotypic divergence of both species, making it appropriate to refer to both species as co-mimics. However, evidence from Symula, Schulte, and Summers (2003) indicates that, in this mimicry system, divergence between the model species preceded divergence between *R. imitator* morphs, making it appropriate to use the terms “model” and “mimic” in this case.

Divergence in color pattern in *R. imitator* is associated with geographic distance between the ranges of the model species. The model species are all allopatric with one another, while the range of *R. imitator* expands across all of them. At each location where *R. imitator*’s range overlaps with a different congener, a different color pattern phenotype of *R. imitator* has evolved, matching the common local sympatric model species. To more efficiently train local predators to avoid a single phenotype, selection has favored divergence in color pattern within *R. imitator* and convergence in color pattern between each morph and its model (Yeager et al. 2012).

Narrow transition zones bridge the barriers between the separate ranges of the morphs of *R. imitator* (Twomey et al. 2013). While gene flow still occurs within these transition zones, there is evidence of incipient speciation acting on the varadero morph. Twomey, Vestergaard, and Summers (2014) showed that there is reduced gene flow (as measured by genetic structuring) between the striped and varadero populations, which is associated with reproductive isolation (as measured by mating preferences) between the same populations. Twomey et al. (2016) investigated evidence for incipient speciation in two other *R. imitator* transition zones (striped-spotted and striped-banded). Their results showed that genetic distance in these two transition zones was correlated with geographic distance rather than color pattern distance, which indicates that color pattern divergence is this case has not resulted in a barrier to gene flow. In the transition zones where there is not a barrier to gene flow, admixture likely keeps background genetic divergence low, while positive frequency-dependent selection on mimetic phenotypes likely maintains the differentiated loci.

Our main goal in this project is to investigate candidate loci for an association with skin color pattern phenotype in *R. imitator*. Considerable work has been done in this regard in a similar mimicry system, *Heliconius*, which is a genus of butterflies that lives in the same geographic region as *R. imitator*. This radiation, similar to the one in *R. imitator*, was also caused by local adaptations to predators through Mullerian mimicry (Sheppard et al. 1985) and has similarly led to multiple transition zones (Mallet 1986). Work in *Heliconius* transition zones indicates that there is strong frequency-dependent selection that maintains narrow hybrid zones, with the survival of "unusual" morphs being significantly lower than that of "usual" morphs (Mallet and Barton 1989; Mallet et al. 1990). Work on the genetic basis of mimetic color pattern in *Heliconius* has revealed supergenes consisting of multiple, sometimes pleiotropic, genes controlling wing color pattern (James Mallet and Clarke 1989; Counterman et al. 2010; Jiggins and McMillan 1997; Kronforst and Papa 2015; Saenko et al. 2019; Morris et al. 2019).

In *R. imitator,* our goal is to understand more about the genetic basis of mimetic phenotypes. Recent work by Linderoth et al. (2018) identified candidate genes for color pattern in the striped-banded transition zone of *R. imitator* by employing exome-wide admixture mapping and association analysis methods. In this thesis, I focus on investigating four of the resulting candidate genes (*asip*, *mc1r*, *bsn*, and *retsat*) in a lab-reared pedigree of banded and striped morphs of *R. imitator*. Two of these genes (*mc1r* and *asip*) are classically known for their link with color pattern in various organisms. *Retsat* also has an emerging role in affecting carotenoid-based coloration. *Bsn* is not well known to have roles in color pattern development.

Polymorphisms in the *asip* gene, which codes for the agouti signaling protein, are associated with color pattern variation in sheep (Zhang et al. 2017), coat color in camels (Almathen et al. 2018), and feather color in chickens (Yang et al. 2019). The agouti signaling protein interacts with the melanocortin 1 receptor (coded by *mc1r*) to control the production of pheomelanin (a red-yellow pigment) and eumelanin (a brown-black pigment). The association between *mc1r* and skin/coat coloration has been well established in multiple organisms, including fish (Bar et al. 2013; Mandal et al. 2020), reptiles (Rosenblum, Hoekstra, and Nachman 2004; Corso, Gonçalves, and de Freitas 2012; Cox, Rabosky, and Chippindale 2013), birds (Doucet et al. 2004, Yang et al. 2019), mice (Nachman, Hoekstra, and D'Agostino 2003; Wada, Okumoto, and Tsudzuki 1999), and humans (Makova and Norton 2005; Valverde et al. 1995).

There is also emerging evidence for *retsat* as a color gene in the literature. The *retsat* gene codes for the retinol saturase protein, which is an oxidoreductase enzyme expressed in metabolically active tissues. In humans, it affects adipocyte differentiation, lipid (retinol) metabolism, and macrophage function among other things (Weber et al. 2020). With respect to coloration, the *retsat* gene has been identified as a candidate color gene in fish, being more highly expressed in orange/yellow vs white skin (Salis et al. 2019; Ahi et al. 2020). The target of the retinol saturase enzyme, vitamin A1 (aka retinol), was shown to mediate the effect of beta-

carotene on coloration in lacertid lizards (San-Jose et al. 2013). In other organisms, like birds, beta-carotene is known to affect yellow to red plumage coloration (Lopes et al. 2016; Hudon et al. 2015). If retinol affects carotenoid-based coloration in *R. imitator*, the retinol saturase enzyme may be an important mediator of that process.

The *bsn* gene codes for the Bassoon protein, which, in humans, is expressed mainly in the neurons of the brain. It is a scaffolding protein involved in the organization of the presynaptic cytoskeleton (Richter et al. 1999). Its role in color pattern development is unclear despite strong evidence from the exon capture study making it a candidate for controlling color pattern in this species.

In this thesis, I tested these four candidate genes (*asip*, *mc1r*, *retsat* and *bsn*) within a lab-reared pedigree of striped and banded *R. imitator*. There are a few notable differences between the striped and banded morphs of *R. imitator* (Figure 1). As their names suggest, banded individuals have horizontal bands across their dorsum, while striped individuals have vertical stripes along their dorsum. Their coloration is different, with banded frogs having an orange dorsum with orange legs and striped individuals having a yellow dorsum with blue/green legs.

Figure 1. Banded (left) and striped (right) morphs of *R. imitator*.

In addition to testing these genes for an association with skin color pattern in *R. imitator*, I also tested for signals of positive selection acting on them. Because aposematic traits are typically under positive-frequency dependent selection, we expect that there is positive selection acting on the loci associated with skin color pattern. By investigating these genes in these contexts, we can understand more about the evolution of skin color pattern in this species.

METHODS

Captive Frog Colony

To form our captive colony of *Ranitomeya imitator*, we procured individuals from known localities in Peru from Understory Enterprises, a licensed supplier. Our frog colony consists of those frogs that we procured as well as their offspring, which we bred. We maintained our frog colony in a temperature-controlled room in the basement of Howell Science Complex at East Carolina University. We keep the lights in the room on a 12-hour light-dark cycle to maintain regular circadian rhythms. *Ranitomeya imitator* is a diurnal species, so the lights are programmed to be on for 12 hours from the early morning until the evening, after which they turn off until the next day. Adult frogs are kept in vivaria containing sphagnum moss as substrate along with a coconut husk hide and pothos plants. Vivaria containing breeding pairs also contain two capped PVC pipes containing water, which serve as egg deposition sites. Frog vivaria are misted regularly to maintain proper humidity. Adult frogs are fed ~10-15 wingless fruit flies each, 3 times per week. Tadpoles are fed tropical fish food twice a week, and once metamorphosed, small juveniles are fed a constant diet of springtails until they become large enough to eat fruit flies. Fruit fly and springtail populations are maintained within the lab. All animal use procedures necessary for this study were approved by the Institutional Animal Care and Use Committee at East Carolina University (AUP: D281a).

Pedigree Formation/Breeding

Breeding was monitored twice a week, and offspring were removed from breeding pools once they could swim freely (Gosner stage 26-30). After removal from breeding pools, tadpoles were given unique identification numbers and kept individually in small plastic cups filled with water until they developed forelimbs (Gosner stage 42). They were then moved to square plastic water-filled containers, which were tilted to provide a dry platform for the metamorph to use as it became terrestrial. Offspring containers were converted to terrestrial vivariums (i.e. moss substrate was added) once metamorphs fully resorbed their tail (Gosner stage 46).

We formed our pedigree by crossing banded and striped parental individuals, then crossing F1s to produce F2s. The parental generation in our pedigree comprises six individuals (three striped and three banded). We crossed banded males with striped females (and vice versa) to produce multiple F1 offspring for each cross. We then paired a female F1 from one cross with a male F1 from another cross multiple times to form multiple pairs, which each produced multiple F2 offspring (Figure 2). Our pedigree consists of 82 total individuals, of which we had six parentals, 14 F1s, and 62 F2s.

Genotyping

For genotyping, we collected a single toe clip from each frog in our multi-generational pedigree. Toe clips were individually submerged in ethanol and stored in separate eppendorf tubes at -80°C. Before DNA extraction, we soaked toe clips in ultrapure water overnight to remove any residual ethanol. We isolated genomic DNA from the toe clips using a DNeasy Blood & Tissue kit from Qiagen. Once the DNA was isolated, we performed gel electrophoresis for each sample to ensure DNA quality. To amplify candidate gene regions containing focal loci, we performed PCR for each sample using oligonucleotide primers designed by Tyler Linderoth using genomic DNA from the exome capture libraries (Linderoth et al. 2018). Following PCR amplification, we performed gel electrophoresis as a quality check to ensure that gene amplification was successful. Before submitting samples for sequencing, we purified the PCR product using one of two ThermoFisher Scientific kits: Exo-Sap-It or GeneJET. If purified with GeneJET, we then quantified DNA concentration and diluted samples if necessary. If purified with Exo-Sap-It, we proceeded straight to sequencing. Gene regions were sequenced in both forward and reverse directions on an Applied Biosystems SeqStudio Genetic Analyzer at the ECU Genomics Core Facility. We used Geneious v11.1.5 to view and analyze resulting electropherogram files. For each gene region in each individual, we aligned forward and reverse sequences using the Geneious sequence alignment algorithm, which is a progressive pairwise aligner similar to ClustalW. We then trimmed base calls having an error probability greater than 0.05 and extracted consensus

sequences. Finally, we searched for the motifs containing the polymorphic loci of interest. This allowed us to determine the genotype of each individual at each polymorphic site.

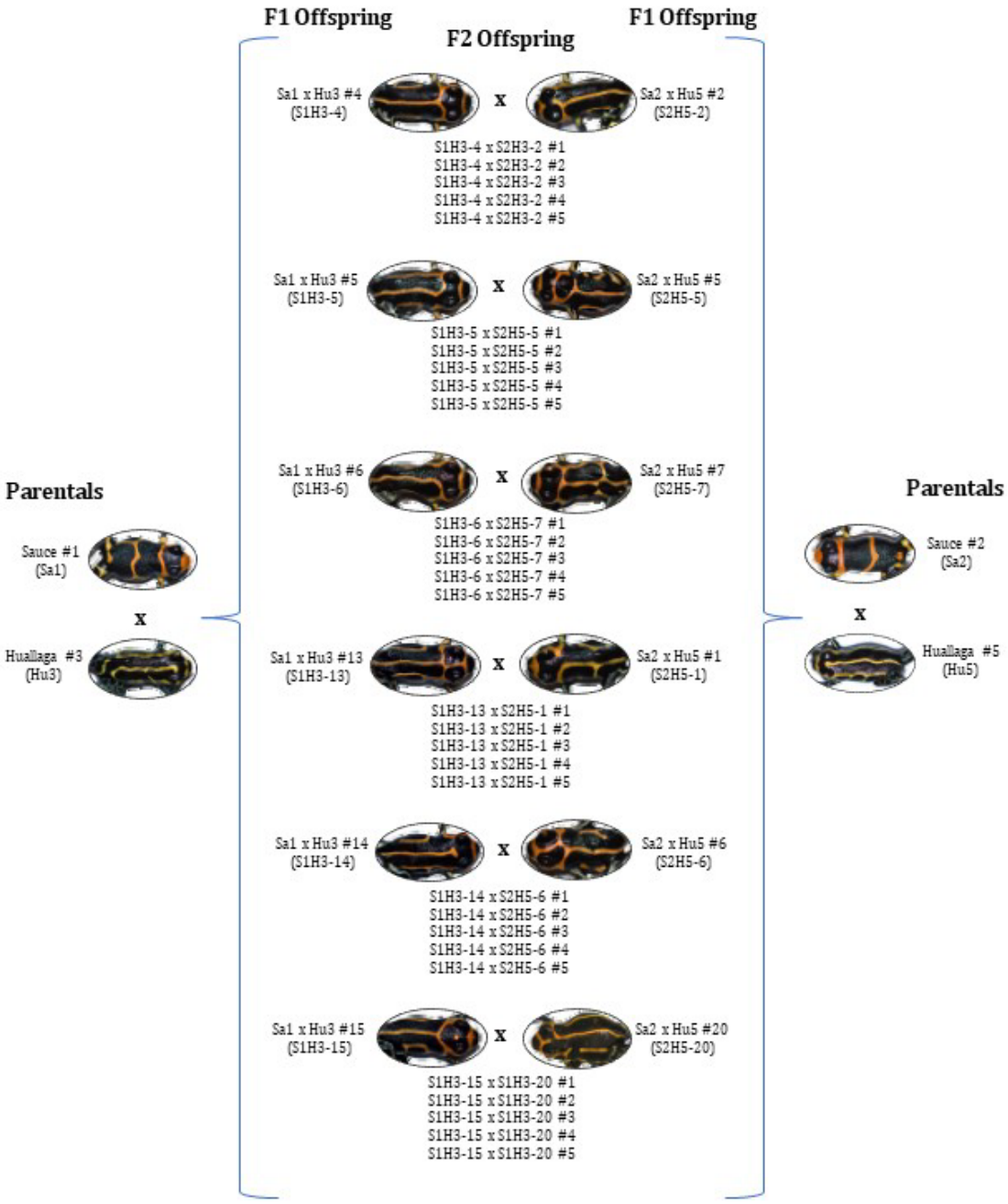

Figure 2. Diagram of our lab-reared pedigree. On the far left and far right, two of the parental crosses are shown. Within the brackets are the resulting F1 crosses with a sample of their offspring (F2s) below. Note: this diagram does not contain all 82 frogs in the pedigree.

Color Phenotyping

To collect spectral reflectance data, we used an Ocean Optics USB spectrometer and the associated Ocean Optics software. We collected 15 data points (8 dorsal, 4 limbs, 3 ventral) for each frog. The data points are outlined in figure 3. We calibrated the spectrometer with a pure white standard between each frog to maintain the accuracy of the measurements.

We used the "pavo" package in R to visualize, clean, and analyze the resulting spectral reflectance data (Maia et al. 2019). The code can be found in our github repository at https://github.com/ksummers26/pavo-code.git. We first subdivided the data into groups with reference to body region, as shown in figure 3. For each region (dorsal and hindlimb) on each frog, we aggregated the data points by taking the mean, and we fixed negative values by setting them to zero. Visualization showed noise at both ends of the spectral curve. To control for that, we truncated the spectra to a wavelength range of 450 - 950 nm (previously 400 - 1041 nm). After processing the spectral reflectance data, we visualized them again, this time with the average and standard deviation plotted.

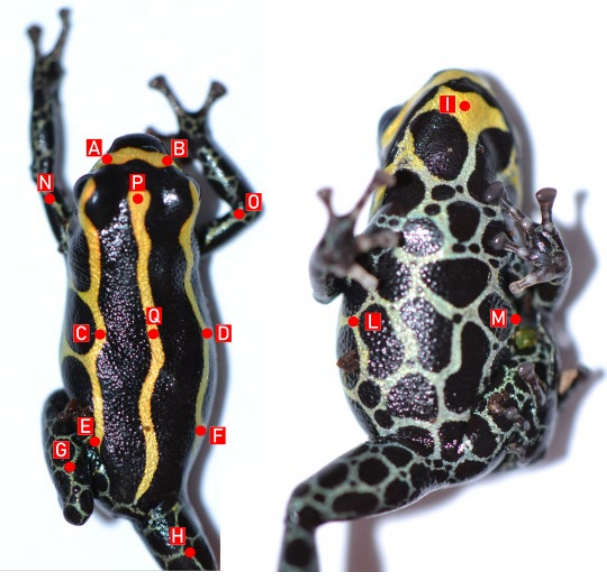

Figure 3. Diagram showing the distribution of spectral reflectance measurements taken from each frog. For analysis, data points were combined into two groups: dorsal measurements (a, b, c, d, e, f, p, and q) and hindlimb measurements (g and h).

We chose four color variables of interest: mean brightness (B2), and relative contribution of green, yellow, and red wavelengths to total brightness (S1G, S1Y, and S1R respectively). Mean brightness (B2) was chosen instead of total brightness across the spectral range because values of mean brightness are more comparable across studies. Chroma measures S1G, S1Y, and S1R were chosen because we expect coloration within the striped-banded cross to differ mainly within the yellow to red wavelengths for the dorsum and green to red wavelengths for the limbs. We used three summary color variables for each body region (B2, S1Y, S1R for the dorsum, and B2, S1G, S1R for the hindlimbs). See Figure 4 for further explanation of these variables.

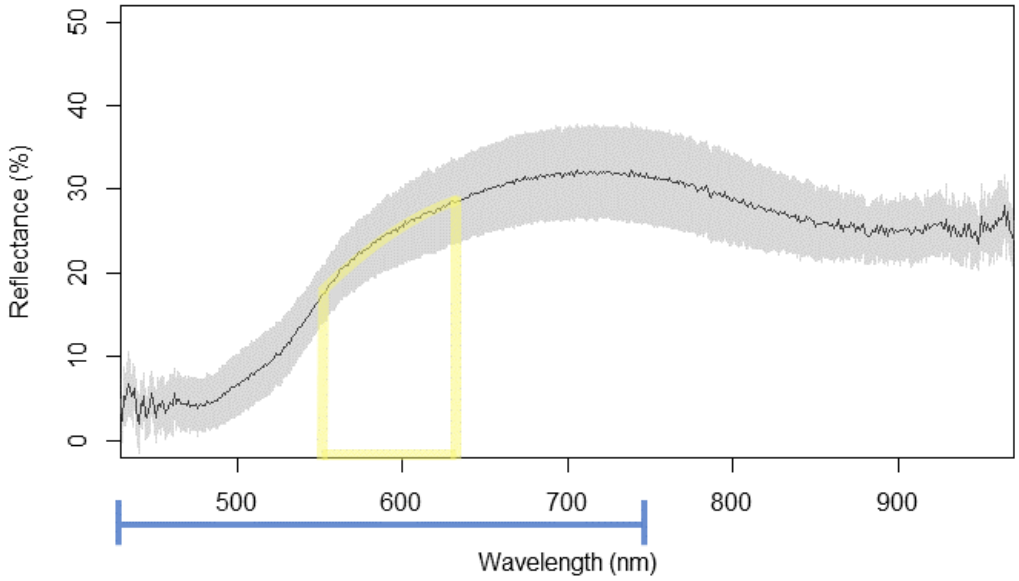

Figure 4. Example of a spectral reflectance curve and diagram of summary color variables. The blue line under the x-axis indicates the human-visible color spectrum. The solid black line and the gray area surrounding it indicate the mean spectral reflectance and standard deviation. Chroma values (S1R, S1Y, S1G) are measured as the contribution of certain wavelengths (red, yellow, and green, respectively) to total brightness. Total brightness is measured as the area under the curve. The contribution of yellow wavelengths, for example, is measured as the area within the yellow polygon divided by the total area under the curve. Mean brightness (B2) is not shown on this diagram; it is the average reflectance value over the entire spectral range.

Pattern phenotyping

To measure pattern phenotype, we followed the methods described in Linderoth et al (2018), which measures the orientation of dorsal stripes/bands. Rotation scores are measured relative to the horizontal axis. Scores greater than zero indicate angles greater than 45 degrees (i.e. more striped), whereas scores below zero indicate angles less than 45 degrees (i.e. more banded).

Genetic Association Analysis

The association analysis was performed using the Merlin program (Abecasis et al. 2002). We used the default settings, aside from changing the complexity threshold to allow more complex (larger) families. We tested for an association with dorsal pattern (rotation score) for all four genes. Because color variables were associated (see Figure 5), we used a hierarchical system to test them. We tested dorsal and hindlimb brightness first. If we did not find a statistically significant association with dorsal or hindlimb brightness and the previous study by Linderoth et al. (2018) indicated a link between them, we performed subsequent tests of chroma variables in order to thoroughly test for an association with color. Association analyses were performed separately for each body region and gene using the --assoc option, which performs a likelihood ratio test to assess the likelihood of observing the data, assuming no association between genotype and phenotype. LOD scores were calculated by taking the log of the odds ratio of the observed distribution versus a distribution with no genotype-phenotype association. A positive LOD score indicates that allele sharing among individuals with similar phenotypes is higher than expected, assuming no association between genotype and phenotype.

Control of False Discovery Rate

When multiple significance tests are performed, the likelihood of obtaining a type I error (i.e. an incorrect rejection of the null hypothesis, or a false discovery) increases (Benjamini and Hochberg 1995). False discovery rate (FDR) controlling procedures, which control the expected proportion of type I errors, are less stringent than familywise error rate controlling procedures

(like the Bonferroni correction), which control for the probability of at least one false discovery. Thus, controlling the FDR is a more powerful approach to detect a true association than controlling familywise error rate. Our genetic association analysis resulted in a total of 19 significance tests. We used the Benjamini-Hochberg (BH) procedure to control the false discovery rate to 0.1 for these tests (Benjamini and Hochberg 1995). An assumption of this procedure is that all tests are independent. Since some phenotypes are correlated (see correlations in Figure 5 below), our tests are not independent. Using this method for non-independent tests increases the proportion of rejected hypotheses, making it more conservative (van Loon 2017).

Tests for Positive Selection

We used codeml (a PAML program) to estimate rates of synonymous and nonsynonymous substitution and detect positive selection in the protein-coding DNA sequences of each candidate gene (Yang 2007). CODEML implements maximum-likelihood models to investigate signals of selection at the branch and codon levels within a phylogenetic framework. We gathered *mc1r*, *asip*, *bsn*, and *retsat* sequences for other organisms by performing BLASTX searches using *R. imitator* nucleotide sequences as queries. The searches were performed using default parameters. We selected all resulting amphibian amino acid sequences for each gene, along with the corresponding nucleotide sequences. We also gathered sequences from two outgroup taxa for each gene. Additionally, we converted several dendrobatid transcriptomes to BLAST-searchable databases, which allowed us to identify orthologous nucleotide sequences for closely related organisms which are not in the NCBI database. We translated these sequences into protein sequences using Geneious. Once all sequences had been gathered, we aligned all nucleotide and protein sequences, separately, for each gene using the Geneious alignment. We then used PAL2NAL to construct a multiple codon alignment from the protein and nucleotide alignments for each gene (Suyama, Torrents, and Bork 2006). To construct the phylogenetic trees for use in the CODEML analysis, we used recent phylogenetic summaries by Hime et al. (in press), Guillory et al. (2019) and the 2019 Amphibian Family Phylogeny published on

amphibiaweb.org. The trees used for analysis were unrooted, as required by the CODEML program, by forming a tritomy between the amphibians and the two outgroups.

As a measure of selection, CODEML quantifies the ratio of non-synonymous to synonymous nucleotide substitutions (ω). Under neutral evolution, ω is expected to be equal to 1. Positive selection is indicated by an ω value greater than 1, and negative (purifying) selection is indicated by a ω value less than 1. CODEML implements site-specific models and branch-specific models, which can be used to identify selection on specific codons and branches (lineages), respectively. We used both in this study. Before testing for selection, we ran model M0, which only allows one ω, to estimate branch lengths on our trees, which we used for all subsequent analyses. Due to the number of tests necessary for this project, we used the LMAP pipeline, which provides a streamlined method for performing multiple CODEML runs (LMAP: http://lmapaml.sourceforge.net/).

We first used codon-specific models to test for selection across the phylogeny. We used two pairs of models: M1a (model with $0<\omega<1$) and M2a (model with $\omega>1$), and M7 (model assuming beta distribution of ω, with $0<\omega<1$) and M8 (model assuming beta distribution of ω, $\omega>1$). We used likelihood ratio tests to compare the results of the models that allowed positive selection (M2a and M8) to the tests that did not allow positive selection (M1a and M7). Evidence for positive selection is indicated if M2a provides a better fit for the data than M1a or if M8 provides a better fit than M7. To determine the model that best fits the data (M1a vs M2a or M7 vs M8), we performed a likelihood ratio test by taking the difference in the loglikelihood estimates and multiplying by two ($2\Delta l$). We used the χ^2 distribution to test for significance, which makes the test conservative, especially with short or very similar sequences (Anisimova, Bielawski, and Yang 2001). With df=2 and p=0.05, the chi-square critical value is 5.9915. If the difference in likelihoods ($2\Delta l$) is greater than or equal to 5.9915, we can infer that the model that allows positive selection is a better fit for the data than the model that does not allow positive selection, thus providing evidence for positive selection. The test of M1a vs M2a is more

stringent than M7 vs M8. For genes that showed evidence of positive selection, we carried out several runs with varying values for kappa (0.5, 2, 5) to ensure that the models had not converged on a local maximum, leaving a global maximum undetected. The resulting likelihoods were compared and the highest one was taken as the best estimate. Posterior probabilities of selection on each codon were estimated using the Bayes Empirical Bayes method.

For branch-site-specific analysis, we used Models A and Afix, which detect selection on specific codons and along specified branches of a phylogenetic tree. We used these models to test for selection acting at the Dendrobatidae (family), *Ranitomeya* (genus), and *Ranitomeya imitator* branches. Models A and Afix separate site classes into different levels (0, 1, 2a, and 2b) depending on the level of selection acting on them. Site class 0 includes codons that are conserved throughout the tree ($0<\omega<1$). Site class 1 includes codons that are evolving neutrally throughout the tree ($\omega =1$). Site classes 2a and 2b include codons that are conserved (2a) or neutral (2b) on the background branches but are under positive selection ($\omega>1$) on the foreground branches (Zhang et al. 2005). Model Afix provides a point of comparison for Model A by fixing ω at 1 for the foreground branches in site classes 2a and 2b, thus disallowing positive selection on the branches/sites being tested. To determine the model that best fits the data, we performed a likelihood ratio test as above. In this case, df=1, so the chi-square critical value for a significance level of 0.05 is 3.8415. As above, posterior probabilities of selection on each codon were estimated using the Bayes Empirical Bayes method.

RESULTS

Genotyping

We determined 81 *mc1r*, 80 *asip*, 80 *bsn*, and 62 *retsat* genotypes with an average of 2x coverage for each. Table 1 outlines the genotypes for pure morph individuals (Huallaga=striped, Sauce=banded). Three of the four polymorphisms (*retsat*, *bsn*, and *asip*) resulted in an amino acid differences within the coding sequences of the genes. Table 2 shows the counts and percentages of each genotype for each gene.

Genotype at Locus of Interest

Genes	Huallaga (Striped) Morph	Sauce (Banded) Morph
Mc1r	CC	TT
Asip	CC	TT
Bsn	AA	CC
Retsat	CT	TT

Table 1. Genotypes of pure morphs at the loci of interest in each gene.

Number (%) of Individuals with Genotype

Genes	Homozygous Huallaga-like	Heterozygous	Homozygous Sauce-like
Mc1r	18 (22%)	42 (52%)	21 (26%)
Asip	12 (15%)	56 (70%)	12 (15%)
Bsn	14 (18%)	45 (56%)	21 (26%)
Retsat	N/A	16 (26%)	46 (74%)

Table 2. Number of individuals of each genotype at each of the four gene loci.

Color and Pattern Phenotyping

We quantified coloration using spectral reflectance measurements from 73 individuals in the pedigree. Aside from dorsal brightness (B2_dors) and yellow chroma (S1Y_dors), pairwise linear regressions indicated statistically significant correlations between all measured color variables within each body region (Figure 5). Due to these correlations, we used a hierarchical approach to test color phenotypes within body regions, prioritizing B2, then moving to chroma variables if necessary. Once we found statistically significant evidence for an association between

a gene and a color variable within a body region, no subsequent tests of color variables were performed for that gene in that body region.

Pattern was quantified for 64 individuals in the pedigree. We found two weak negative correlations between pattern and dorsal color variables (B2 and S1R). These indicate that a lower (i.e. more banded) rotation score is correlated with higher mean brightness and higher contribution of red wavelengths to overall brightness. This correlation could be due to pleiotropy of genes controlling color and pattern.

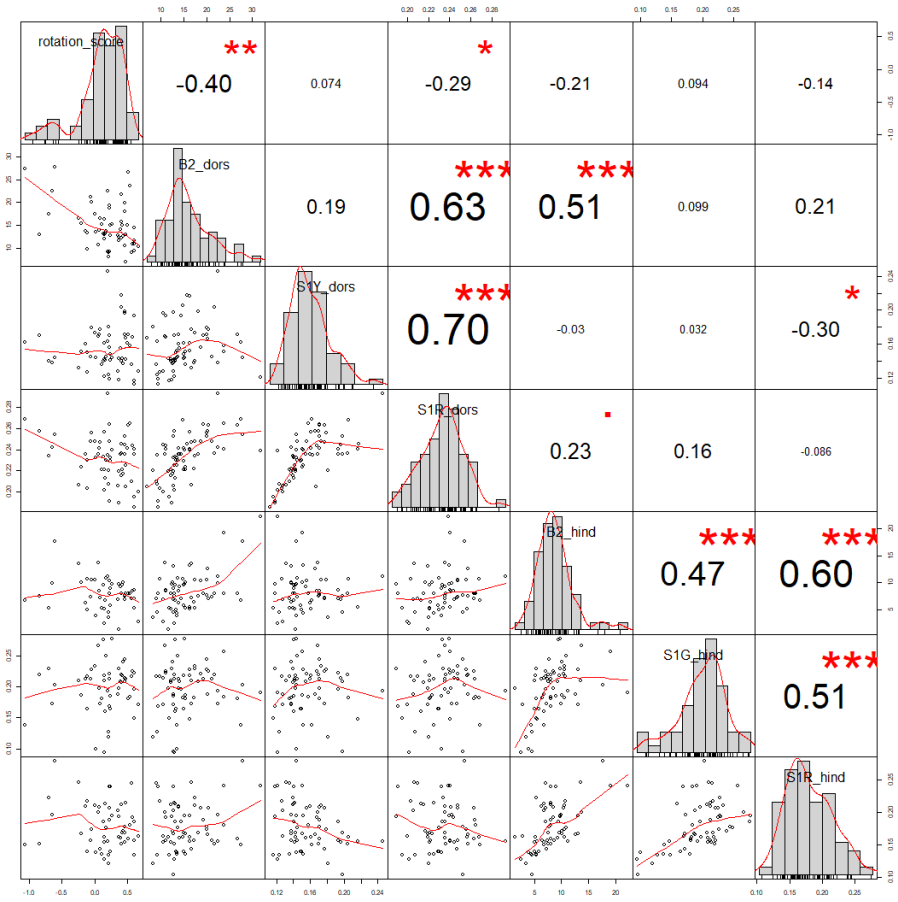

Figure 5. Correlation matrix of phenotypic variables. Histograms of variables are aligned along the diagonal. Bivariate scatterplots are shown below the diagonal with a fitted line in red. Each point on the scatterplot represents a measurement from one individual. Pearson correlation coefficients and level of significance are shown above the diagonal (. = p<0.10 * = p<0.05, ** = p<0.005, *** = p<0.001).

Association analysis

We found evidence for association between phenotype and genotype for all four of the loci we tested (Table 3). All of these (except the association between *bsn* and color pattern) were still statistically significant after performing adjustments for false discovery rates.

Gene	Associated Phenotype	LOD score	P-value	P-value Rank	BH-critical value
Mc1r	Pattern	2.52	0.00066	3	0.016
	Hindlimb Color (B2)	1.17	0.020	5	0.026
Asip	Pattern	2.54	0.00062	2	0.011
	Dorsal Color (B2)	2.47	0.00075	4	0.021
Retsat	Pattern	1.10	0.024	6	0.032
	Dorsal Color (S1Y)	3.77	0.000031	1	0.005
Bsn	Pattern	0.93	0.039	7	0.037

Table 3. Summary of association tests with lowest p-values. LOD score indicates the amount of allele-sharing between individuals with similar phenotypes. A higher LOD score indicates more allele sharing. The BH-critical values are calculated by dividing the p-value rank by the total number of tests (19) and multiplying by the false discovery rate (0.1). For tests with p-values lower than the BH-critical value, we fail to reject the null hypothesis.

Key results for each gene are summarized below and in Figure 6.

***Asip*-** Individuals with a Huallaga-like CC genotype for *asip* had a higher (more striped) rotation score (LOD=2.54, p=0.00062) and lower dorsal brightness (LOD=2.47, p=0.00075).

***Bsn*-** Individuals with the AA (Huallaga-like) genotype for *bsn* had a higher rotation score (LOD=0.93, p=0.039).

***Mc1r*-** Individuals with a Huallaga-like CC genotype for *mc1r* had a higher rotation score (LOD=2.52, p=0.00066) and lower hindlimb brightness (LOD=1.17, p=0.02).

***Retsat*-** Individuals with a Sauce-like TT genotype had a lower rotation score (LOD=1.10, p=0.024) and lower contribution of yellow wavelengths to dorsal brightness (LOD=3.77, p=0.000031).

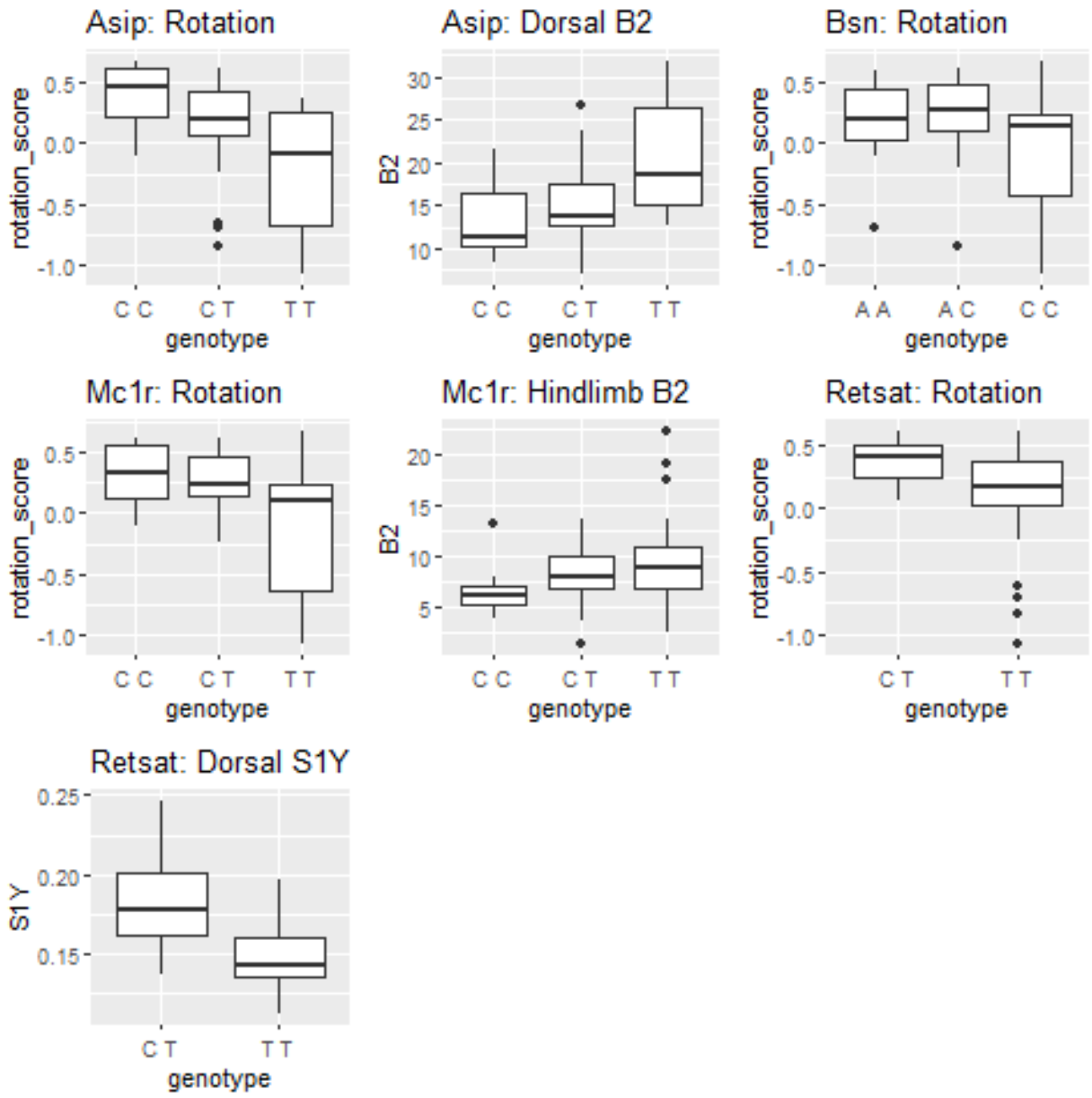

Figure 6. Boxplots of genotype vs phenotype for each association. Rotation scores were higher (more striped) for individuals with Huallaga-like genotypes across all four genes. Dorsal brightness and hindlimb brightness were higher for those with a Sauce-like *asip* and *mc1r* genotypes, respectively. Individuals with a Sauce-like genotype for *retsat* had a lower contribution of yellow wavelengths to their total dorsal brightness.

All four candidate genes tested in this study had an association with rotation score; individuals with a Huallaga-like genotype had higher (i.e. more striped) rotation scores. At all four loci, heterozygous individuals had rotation scores that were more like striped Huallaga individuals than banded Sauce individuals, suggesting dominance of the "striped" alleles. Additionally, *asip* and *mc1r* had significant associations with dorsal and hindlimb brightness, respectively. Individuals with a Sauce-like genotype for *asip* and *mc1r* had a higher mean brightness that those with Huallaga-like genotypes. For *retsat*, individuals with a Huallaga-like genotype had a higher contribution of yellow wavelengths to total brightness. Aside from *retsat*, which only had two genotypes, color measurements for heterozygous individuals were intermediate, which suggests incomplete dominance of color alleles.

Signals of Selection

Our blast searches resulted in 10-15 orthologous from other amphibians for each gene (Table 4).

Gene	**Organisms**
Mc1r	*Alligator mississippiensis, Dendrobates auratus, Gavialis gangeticus, Nanorana parkeri, Oophaga histrionica, Oophaga pumilio, Oophaga sylvatica, Rana arvalis, Rhinatrema bivittatum, Ranitomeya fantastica, Ranitomeya imitator, Ranitomeya summersi, Rana temporaria, Ranitomeya variabilis, Xenopus laevus, Xenopus tropicalis*
Asip	*Andrias davidianus, Dendrobates auratus, Lacerta agilis, Nanorana parkeri, Oophaga pumilio, Podarcis muralis, Rhinatrema bivittatum, Ranitomeya fantastica, Ranitomeya imitator, Ranitomeya variabilis, Xenopus tropicalis*
Bsn	*Dendrobates auratus, Gavialis gangeticus, Gekko japonicus, Geotrypetes seraphini, Microcaecilia unicolor, Nanorana parkeri, Oophaga pumilio, Rhinatrema bivittatum, Ranitomeya imitator, Xenopus tropicalis*
Retsat	*Dendrobates auratus, Geotrypetes seraphini, Microcaecilia unicolor, Nanorana parkeri, Oophaga pumilio, Podarcis muralis, Rhinatrema bivittatum, Ranitomeya fantastica, Ranitomeya imitator, Ranitomeya summersi, Ranitomeya variabilis, Terrapene carolina, Xenopus laevis, Xenopus tropicalis*

Table 4. Organisms with sequences identified from blast searches used in CODEML analysis. All are amphibains, aside from the two outgroups per gene, which are underlined.

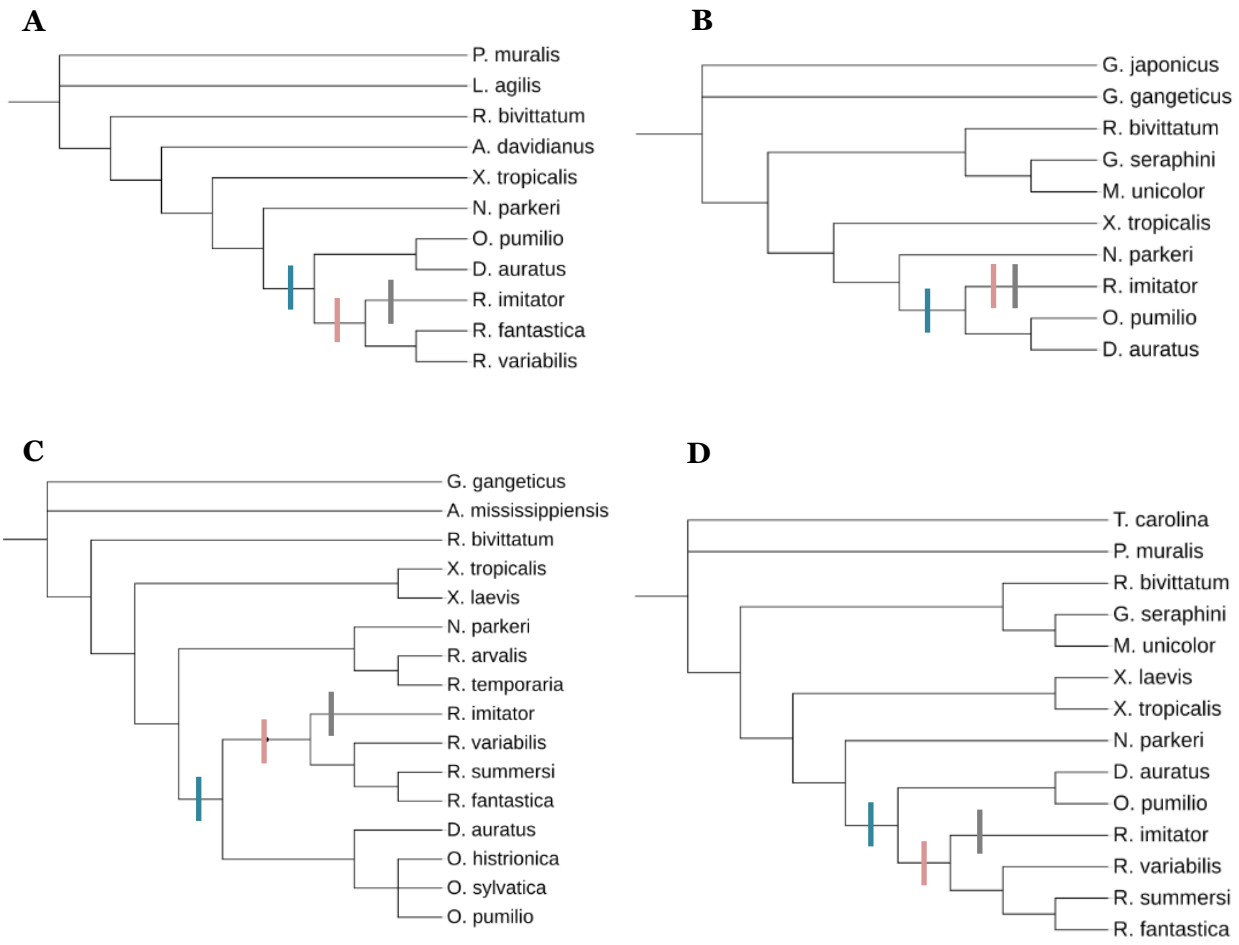

Figure 7. Phylogenetic trees used in CODEML analyses of the **A)** *asip*, **B)** *bsn*, **C)** *mc1r*, and **D)** *retsat* genes. Bars denote the specific lineages we tested for positive selection (blue = Dendrobatidae family, red = *Ranitomeya* genus, gray = *Ranitomeya imitator* species).

Tests for positive selection on specific branches (Figure 7) did not result in statistically significant results, suggesting that these genes are not under positive selection at the branch level for the branches tested. However, we did find some evidence of positive selection at specific sites along certain branches for each gene (Table 5). The site with the strongest evidence for positive selection was site 50 in the *bsn* gene (prob(ω>1)=0.903). None of these sites included the loci of interest in this study. In the site models, which test selection across the phylogeny, we did not find any evidence for positive selection. As mentioned above, likelihood ratio tests using

the chi-square distribution are very conservative with respect to identifying positive selection, especially with short or very similar sequences (Anisimova, Bielawski, and Yang 2001). The lengths (in nucleotides) of the sequences we tested were 141 (*asip*), 144 (*retsat*), 483 (*bsn*), and 669 (*mc1r*). For *asip* and *retsat* especially, our results may be limited by the length of the sequence that was tested. Additionally, tests with a greater number of species have more power (Anisimova, Bielawski, and Yang 2001). As such, the tests for *bsn* and *asip* may have been limited by the small number of sequences used.

Gene	**Branch (Foreground Lineage)**	**AA Position**	**BEB Prob(ω>1)**
Asip	Dendrobatidae	38	0.674
Bsn	Dendrobatidae	61	0.553
Bsn	*Ranitomeya imitator*	48, **50**, 60	0.792, **0.903**, 0.746
Mc1r	Dendrobatidae	52, 101, **107**	0.850, 0.637, **0.865**
Mc1r	*Ranitomeya imitator*	58, 115, 171	0.819, 0.836, 0.831
Mc1r	*Ranitomeya*	80	0.846
Retsat	Dendrobatidae	14	0.630

Table 5. Sites with some evidence of positive selection on foreground lineages. Bayes Empirical Bayes posterior probabilities are listed. Typically, sites with a posterior probability greater than 0.95 are considered to be under selection. The sites with the highest posterior probabilities are in bold.

DISCUSSION

Color pattern is mediated by diverse mechanisms, which may involve proteins coded by numerous genes. In the case of *Ranitomeya imitator*, we have identified four genes that show strong evidence of association with skin color and/or pattern. With respect to skin color, we see that polymorphisms in the *asip* and *mc1r* genes, which are associated with melanistic coloration in other organisms, are associated with differences in dorsal and hindlimb brightness in *R. imitator*. *Retsat*, which mediates yellow-red carotenoid coloration in other organisms, is strongly associated with the contribution of yellow wavelengths to dorsal brightness within this pedigree. Additionally, all four genes tested show associations with dorsal patterning in this species, with *mc1r* and *asip* being the most highly associated. These two genes, especially, are known to regulate pattern formation in other species.

In humans and mice, the *asip* gene codes for the agouti signaling protein, which binds to the melanocortin 1 receptor and is a key regulator of melanogenesis. The agouti signaling protein functions to block the binding of alpha-melanocyte-stimulating hormone (alpha-MSH) to the melanocortin 1 receptor, which begins a cascade of reactions that eventually lead to the production of the red-yellow pigment pheomelanin instead of the brown-black pigment eumelanin (Suzuki et al. 1997). When *asip* is not bound to the melanocortin 1 receptor, binding of alpha-MSH is not inhibited, and production of eumelanin is favored. In *R. imitator*, we see evidence that variation in the *asip* and *mc1r* genes is associated with variation in dorsal and hindlimb brightness, respectively. One possible explanation for this is that the single amino acid difference in the agouti signaling protein changes its affinity to the melanocortin 1 receptor, thus causing changes to skin brightness. Since the SNP in *mc1r* does not confer an amino acid change, it is not likely that it affects the function of the melanocortin 1 receptor. However, this SNP could be linked with a change elsewhere in the *R. imitator* genome, potentially in a regulatory region that leads to a difference in mc1r expression or (possibly) in another gene that interacts with *mc1r*.

The *retsat* gene codes for the retinol saturase enzyme. In humans, it has been shown to be involved in lipid metabolism, specifically vitamin A1 (retinol) and carotenoid metabolism. It is not classically known to affect color pattern. However, there is an emerging role for *retsat* as a color gene in brightly colored fish and lizards. A study by Salis et al. (2019) found differential expression in the *retsatl* gene (a *retsat* homolog) between orange and white skin of clownfish. In cichlid fish, *retsatl* has also been revealed as a candidate carotenoid color gene and is differentially expressed in white vs yellow skin of *T. duboisi Maswa* (Ahi et al. 2020). In both species of fish, *retsat* was more highly expressed in orange/yellow skin than white skin. If that differential expression is linked with higher activity of retinol saturase in the orange/yellow skin, the difference in skin coloration may be caused by a difference in carotenoid metabolism. In lacertid lizards, retinol was shown to mediate the effects of beta-carotene on coloration (San-Jose et al. 2013). In the case of *R. imitator*, a single amino acid change in *retsat* was associated with a difference in the contribution of yellow wavelengths to dorsal brightness, which could be caused by functional differences in the effectiveness of the retinol saturase enzyme, which may in turn act on retinol to mediate carotenoid coloration.

All four genes tested in this study were associated with differences in skin patterning. *Asip* and *mc1r* had the strongest evidence for association, with LOD scores above 2.5. These genes are well known in other species to affect skin/coat pattern. In mice, adaptive melanic color pattern is associated with the mc1r gene. (Nachman, Hoekstra, and D'Agostino 2003). Additionally, melanocytes have been shown to mediate pigmentation patterning through *asip* and *mc1r* in the Japanese quail (Inaba et al. 2019). There may be a similar mechanism for patterning in *R. imitator*. This should be investigated.

Bsn and *retsat* also show associations with skin patterning. This is the first evidence of an association of this sort, as there is no published research linking these genes with skin patterning. In humans, the *bsn* gene is known to code for the bassoon protein, which is a scaffolding protein used in the presynaptic cytomatrix of the brain (Richter et al. 1999). Little is

known about the function of the bassoon protein in poison frogs. While this gene did not show a significant association with pattern after controlling for false discoveries in this study, it did trend toward significance, and it showed a high probability of association in the admixture mapping/divergence analysis done by Linderoth et al. (2018). This gene would be a good candidate for a knock-out or knock-down study to investigate more about its function(s) in *R. imitator*. The function of *retsat* is also not very well known in poison frogs. While our results show significant evidence for *retsat* as a potential mediator of color pattern, the study done by Linderoth et al (2018) did not identify it as a candidate gene affecting pattern. From the perspective of those results, in combination with the fact that *retsat* was more highly associated with color than pattern in this study, this gene is a better candidate for coloration than for patterning.

Overall, identifying genes associated with mimetic divergence in this species is key to understanding how it evolved. We have identified and tested four candidate color pattern genes associated with different facets of the mimetic phenotype. While we did not find statistically significant evidence for positive selection acting on these genes, our results are limited due to the length and number of sequences used. Future studies should test these genes in a larger phylogenetic framework. To help elucidate the underlying reasons why these genes are associated with skin color pattern, future studies should investigate the functional roles of these genes in creating color pattern in this species. Further study of these genes will help elucidate the proximate mechanisms of phenotypic divergence in *R. imitator,* giving us a better understanding of the evolution of aposematism in this species and potential insights into the molecular basis of skin color pattern in general.

REFERENCES

Abecasis, Gonçalo R., Stacey S. Cherny, William O. Cookson, and Lon R. Cardon. 2002. "Merlin—Rapid Analysis of Dense Genetic Maps Using Sparse Gene Flow Trees." *Nature Genetics* 30 (1): 97–101. https://doi.org/10.1038/ng786.

Ahi, Ehsan Pashay, Laurène A. Lecaudey, Angelika Ziegelbecker, Oliver Steiner, Ronald Glabonjat, Walter Goessler, Victoria Hois, Carina Wagner, Achim Lass, and Kristina M. Sefc. 2020. "Comparative Transcriptomics Reveals Candidate Carotenoid Color Genes in an East African Cichlid Fish." *BMC Genomics* 21 (1): 54. https://doi.org/10.1186/s12864-020-6473-8.

Almathen, Faisal, Haitham Elbir, Hussain Bahbahani, Joram Mwacharo, and Olivier Hanotte. 2018. "Polymorphisms in MC1R and ASIP Genes Are Associated with Coat Color Variation in the Arabian Camel." *Journal of Heredity* 109 (6): 700–706. https://doi.org/10.1093/jhered/esy024.

Anisimova, Maria, Joseph P. Bielawski, and Ziheng Yang. 2001. "Accuracy and Power of the Likelihood Ratio Test in Detecting Adaptive Molecular Evolution." *Molecular Biology and Evolution* 18 (8): 1585–92. https://doi.org/10.1093/oxfordjournals.molbev.a003945.

Bar, I., E. Kaddar, A. Velan, and L. David. 2013. "Melanocortin Receptor 1 and Black Pigmentation in the Japanese Ornamental Carp (Cyprinus Carpio Var. Koi)." *Frontiers in Genetics* 4 (JAN). https://doi.org/10.3389/fgene.2013.00006.

Benjamini, Yoav, and Yosef Hochberg. 1995. "Controlling the False Discovery Rate: A Practical and Powerful Approach to Multiple Testing." *Journal of the Royal Statistical Society: Series B (Methodological)* 57 (1): 289–300. https://doi.org/10.1111/j.2517-6161.1995.tb02031.x.

Corso, J., G.L. Gonçalves, and T.R.O. de Freitas. 2012. "Sequence Variation in the Melanocortin-1 Receptor (MC1R) Pigmentation Gene and Its Role in the Cryptic Coloration of Two

South American Sand Lizards." *Genetics and Molecular Biology* 35 (1): 81–87. https://doi.org/10.1590/S1415-47572012005000015.

Counterman, Brian A., Felix Araujo-Perez, Heather M. Hines, Simon W. Baxter, Clay M. Morrison, Daniel P. Lindstrom, Riccardo Papa, et al. 2010. "Genomic Hotspots for Adaptation: The Population Genetics of Müllerian Mimicry in Heliconius Erato." *PLOS Genetics* 6 (2): e1000796. https://doi.org/10.1371/journal.pgen.1000796.

Cox, C.L., A.R.D. Rabosky, and P.T. Chippindale. 2013. "Sequence Variation in the Mc1r Gene for a Group of Polymorphic Snakes." *Gene* 513 (2): 282–86. https://doi.org/10.1016/j.gene.2012.10.065.

Doucet, S.M., M.D. Shawkey, M.K. Rathburn, H.L. Mays Jr., and R. Montgomerie. 2004. "Concordant Evolution of Plumage Colour, Feather Microstructure and a Melanocortin Receptor Gene between Mainland and Island Populations of a Fairy-Wren." *Proceedings of the Royal Society B: Biological Sciences* 271 (1549): 1663–70. https://doi.org/10.1098/rspb.2004.2779.

Guillory, Wilson X., Morgan R. Muell, Kyle Summers, and Jason L. Brown. 2019. "Phylogenomic Reconstruction of the Neotropical Poison Frogs (Dendrobatidae) and Their Conservation." *Diversity* 11 (8): 126. https://doi.org/10.3390/d11080126.

Hime, Paul M., Alan R. Lemmon, Emily C. Moriarty Lemmon, Elizabeth Prendini, Jeremy M. Brown, Robert C. Thomson, Justin D. Kratovil, et al. n.d. "Phylogenomics Reveals Ancient Gene Tree Discordance in the Amphibian Tree of Life." *Systematic Biology*. Accessed May 29, 2020. https://doi.org/10.1093/sysbio/syaa034.

Hudon, Jocelyn, Karen Wiebe, Elena Pini, and Stradi Riccardo. 2015. "Plumage Pigment Differences Underlying the Yellow-Red Differentiation in the Northern Flicker (Colaptes Auratus)." *Comparative Biochemistry and Physiology. Part B, Biochemistry & Molecular Biology* 183 (January). https://doi.org/10.1016/j.cbpb.2014.12.006.

Inaba, Masafumi, Ting-Xin Jiang, Ya-Chen Liang, Stephanie Tsai, Yung-Chih Lai, Randall Bruce Widelitz, and Cheng Ming Chuong. 2019. “Instructive Role of Melanocytes during Pigment Pattern Formation of the Avian Skin.” *Proceedings of the National Academy of Sciences* 116 (14): 6884–90. https://doi.org/10.1073/pnas.1816107116.

Jiggins, C.D., and W.O. McMillan. 1997. “The Genetic Basis of an Adaptive Radiation: Warning Colour in Two Heliconius Species.” *Proceedings of the Royal Society B: Biological Sciences* 264 (1385): 1167–75. https://doi.org/10.1098/rspb.1997.0161.

Kronforst, M.R., and R. Papa. 2015. “The Functional Basis of Wing Patterning in Heliconius Butterflies: The Molecules behind Mimicry.” *Genetics* 200 (1): 1–19. https://doi.org/10.1534/genetics.114.172387.

LInderoth, Tyler Philip. 2018. “Identifying Population Histories, Adaptive Genes, and Genetic Duplication from Population-Scale Next Generation Sequencing.” UC Berkeley. https://escholarship.org/uc/item/5kp4q40k.

“LMAP: Lightweight Multigene Analyses in PAML | BMC Bioinformatics | Full Text.” n.d. Accessed May 27, 2020. https://bmcbioinformatics.biomedcentral.com/articles/10.1186/s12859-016-1204-5.

Loon, Wouter van. 2017. “The Power of the Benjamini-Hochberg Procedure.”

Lopes, Ricardo J., James D. Johnson, Matthew B. Toomey, Mafalda S. Ferreira, Pedro M. Araujo, José Melo-Ferreira, Leif Andersson, Geoffrey E. Hill, Joseph C. Corbo, and Miguel Carneiro. 2016. “Genetic Basis for Red Coloration in Birds.” *Current Biology* 26 (11): 1427–34. https://doi.org/10.1016/j.cub.2016.03.076.

Maia, Rafael, Hugo Gruson, John A. Endler, and Thomas E. White. 2019. “Pavo 2: New Tools for the Spectral and Spatial Analysis of Colour in r.” *Methods in Ecology and Evolution* 10 (7): 1097–1107. https://doi.org/10.1111/2041-210X.13174.

Makova, K., and H. Norton. 2005. “Worldwide Polymorphism at the MC1R Locus and Normal Pigmentation Variation in Humans.” *Peptides* 26 (10): 1901–8. https://doi.org/10.1016/j.peptides.2004.12.032.

Mallet, J., N. Barton, G. Lamas, J. Santisteban, M. Muedas, and H. Eeley. 1990. “Estimates of Selection and Gene Flow from Measures of Cline Width and Linkage Disequilibrium in Heliconius Hybrid Zones.” *Genetics* 124 (4): 921–36.

Mallet, James. 1986. “Hybrid Zones of Heliconius Butterflies in Panama and the Stability and Movement of Warning Colour Clines.” *Heredity* 56 (2): 191–202. https://doi.org/10.1038/hdy.1986.31.

Mallet, James, and Nicholas H. Barton. 1989. “Strong Natural Selection in a Warning-Color Hybrid Zone.” *Evolution* 43 (2): 421–31. https://doi.org/10.2307/2409217.

Mallet, James, and Cyril Clarke. 1989. “The Genetics of Warning Colour in Peruvian Hybrid Zones of Heliconius Erato and H. Melpomene.” *Proceedings of the Royal Society of London. B. Biological Sciences* 236 (1283): 163–85. https://doi.org/10.1098/rspb.1989.0019.

Mandal, B.K., H. Chen, Z. Si, X. Hou, H. Yang, X. Xu, J. Wang, and C. Wang. 2020. “Shrunk and Scattered Black Spots Turn out Due to MC1R Knockout in a White-Black Oujiang Color Common Carp (Cyprinus Carpio Var. Color).” *Aquaculture* 518. https://doi.org/10.1016/j.aquaculture.2019.734822.

Morris, J., N. Navarro, P. Rastas, L.D. Rawlins, J. Sammy, J. Mallet, and K.K. Dasmahapatra. 2019. “The Genetic Architecture of Adaptation: Convergence and Pleiotropy in Heliconius Wing Pattern Evolution.” *Heredity* 123 (2): 138–52. https://doi.org/10.1038/s41437-018-0180-0.

Nachman, Michael W., Hopi E. Hoekstra, and Susan L. D’Agostino. 2003. “The Genetic Basis of Adaptive Melanism in Pocket Mice.” *Proceedings of the National Academy of Sciences* 100 (9): 5268–73. https://doi.org/10.1073/pnas.0431157100.

Richter, Karin, Kristina Langnaese, Michael R. Kreutz, Gisela Olias, Rong Zhai, Henning Scheich, Craig C. Garner, and Eckart D. Gundelfinger. 1999. “Presynaptic Cytomatrix Protein Bassoon Is Localized at Both Excitatory and Inhibitory Synapses of Rat Brain.” *Journal of Comparative Neurology* 408 (3): 437–48. https://doi.org/10.1002/(SICI)1096-9861(19990607)408:3<437::AID-CNE9>3.0.CO;2-5.

Rosenblum, E.B., H.E. Hoekstra, and M.W. Nachman. 2004. “Adaptive Reptile Color Variation and the Evolution of the MC1R Gene.” *Evolution* 58 (8): 1794–1808.

Saenko, S.V., M. Chouteau, F. Piron-Prunier, C. Blugeon, M. Joron, and V. Llaurens. 2019. “Unravelling the Genes Forming the Wing Pattern Supergene in the Polymorphic Butterfly Heliconius Numata.” *EvoDevo* 10 (1). https://doi.org/10.1186/s13227-019-0129-2.

Salis, Pauline, Thibault Lorin, Victor Lewis, Carine Rey, Anna Marcionetti, Marie-Line Escande, Natacha Roux, et al. 2019. “Developmental and Comparative Transcriptomic Identification of Iridophore Contribution to White barring in Clownfish.” *Pigment Cell & Melanoma Research* 32 (3): 391–402. https://doi.org/10.1111/pcmr.12766.

San-Jose, Luis M., Fernando Granado-Lorencio, Barry Sinervo, and Patrick S. Fitze. 2013. “Iridophores and Not Carotenoids Account for Chromatic Variation of Carotenoid-Based Coloration in Common Lizards (*Lacerta Vivipara*).” *The American Naturalist* 181 (3): 396–409. https://doi.org/10.1086/669159.

Sheppard, Philip Macdonald, John Richard George Turner, K. S. Brown, W. W. Benson, M. C. Singer, and John Maynard Smith. 1985. “Genetics and the Evolution of Muellerian Mimicry in Heliconius Butterflies.” *Philosophical Transactions of the Royal Society of London. B, Biological Sciences* 308 (1137): 433–610. https://doi.org/10.1098/rstb.1985.0066.

Suyama, M., D. Torrents, and P. Bork. 2006. “PAL2NAL: Robust Conversion of Protein Sequence Alignments into the Corresponding Codon Alignments.” *Nucleic Acids Research* 34 (Web Server): W609–12. https://doi.org/10.1093/nar/gkl315.

Suzuki, I., A. Tada, M. M. Ollmann, G. S. Barsh, S. Im, M. L. Lamoreux, V. J. Hearing, J. J. Nordlund, and Z. A. Abdel-Malek. 1997. “Agouti Signaling Protein Inhibits Melanogenesis and the Response of Human Melanocytes to Alpha-Melanotropin.” *The Journal of Investigative Dermatology* 108 (6): 838–42. https://doi.org/10.1111/1523-1747.ep12292572.

Symula, R., R. Schulte, and K. Summers. 2003. “Molecular Systematics and Phylogeography of Amazonian Poison Frogs of the Genus Dendrobates.” *Molecular Phylogenetics and Evolution* 26 (3): 452–75. https://doi.org/10.1016/s1055-7903(02)00367-6.

Symula, Rebecca, Rainer Schulte, and Kyle Summers. 2001. “Molecular Phylogenetic Evidence for a Mimetic Radiation in Peruvian Poison Frogs Supports a Müllerian Mimicry Hypothesis.” *Proceedings of the Royal Society of London. Series B: Biological Sciences* 268 (1484): 2415–21. https://doi.org/10.1098/rspb.2001.1812.

Twomey, Evan, Jacob S. Vestergaard, and Kyle Summers. 2014. “Reproductive Isolation Related to Mimetic Divergence in the Poison Frog Ranitomeya Imitator.” *Nature Communications* 5 (1): 4749. https://doi.org/10.1038/ncomms5749.

Twomey, Evan, Jacob S. Vestergaard, Pablo J. Venegas, and Kyle Summers. 2016. “Mimetic Divergence and the Speciation Continuum in the Mimic Poison Frog Ranitomeya Imitator.” *The American Naturalist* 187 (2): 205–24. https://doi.org/10.1086/684439.

Twomey, Evan, Justin Yeager, Jason Lee Brown, Victor Morales, Molly Cummings, and Kyle Summers. 2013. “Phenotypic and Genetic Divergence among Poison Frog Populations in a Mimetic Radiation.” *PLOS ONE* 8 (2): e55443. https://doi.org/10.1371/journal.pone.0055443.

Valverde, P., E. Healy, I. Jackson, J.L. Rees, and A.J. Thody. 1995. "Variants of the Melanocyte–Stimulating Hormone Receptor Gene Are Associated with Red Hair and Fair Skin in Humans." *Nature Genetics* 11 (3): 328–30. https://doi.org/10.1038/ng1195-328.

Wada, A., M. Okumoto, and M. Tsudzuki. 1999. "Tawny: A Novel Light Coat Color Mutation Found in a Wild Population of Mus Musculus Molossinus, a New Allele at the Melanocortin 1 Receptor (Mc1r) Locus." *Experimental Animals* 48 (2): 73–78. https://doi.org/10.1538/expanim.48.73.

Weber, P., R.E. Flores, M.F. Kiefer, and M. Schupp. 2020. "Retinol Saturase: More than the Name Suggests." *Trends in Pharmacological Sciences*. https://doi.org/10.1016/j.tips.2020.03.007.

Yang, C.-W., J.-S. Ran, C.-L. Yu, M.-H. Qiu, Z.-R. Zhang, H.-R. Du, Q.-Y. Li, et al. 2019. "Polymorphism in MC1R, TYR and ASIP Genes in Different Colored Feather Chickens." *3 Biotech* 9 (5). https://doi.org/10.1007/s13205-019-1710-z.

Yang, Ziheng. 2007. "PAML 4: Phylogenetic Analysis by Maximum Likelihood." *Molecular Biology and Evolution* 24 (8): 1586–91. https://doi.org/10.1093/molbev/msm088.

Yeager, Justin, Jason L. Brown, Victor Morales, Molly Cummings, and Kyle Summers. 2012. "Testing for Selection on Color and Pattern in a Mimetic Radiation." *Current Zoology* 58 (4): 668–76. https://doi.org/10.1093/czoolo/58.4.668.

Zhang, J. 2005. "Evaluation of an Improved Branch-Site Likelihood Method for Detecting Positive Selection at the Molecular Level." *Molecular Biology and Evolution* 22 (12): 2472–79. https://doi.org/10.1093/molbev/msi237.

Zhang, Xuemei, Wenrong Li, Chenxi Liu, Xinrong Peng, Jiapeng Lin, Sangang He, Xuejiao Li, et al. 2017. "Alteration of Sheep Coat Color Pattern by Disruption of ASIP Gene via CRISPR Cas9." *Scientific Reports* 7 (1): 1–10. https://doi.org/10.1038/s41598-017-08636-0.